IMPLEMENTATION OF PLASTICITY MODEL FOR A STEEL WITH MIXED CYCLIC SOFTENING AND HARDENING AND ITS APPLICATION TO FATIGUE ASSESSMENTS

Volodymyr Okorokov✉,*, Tugrul Comlekci*, Donald MacKenzie*, Ralph van Rijswick† and Yevgen Gorash*

This paper presents a numerical modelling and experimental investigation of the cyclic plasticity behaviour of low carbon steel. In order to improve the accuracy of modelling the material response under cycling loading, a new set of internal variables is proposed. The developed plasticity model is applied to the problem of modelling compressive residual stress inducing methods which are based on a plastic overload of a material. A beneficial influence of induced compressive residual stress is demonstrated on a benchmark problem of autofrettage of a high pressure thick-walled cylinder. Numerical simulation of the cyclic plasticity problems and fatigue assessments are carried out by means of FEM in ANSYS Workbench with FORTRAN user-programmable subroutines for material model incorporating custom equations.

INTRODUCTION

Nowadays, low carbon steel has become the most popular type of structural steel because of its relatively low price and good material properties, which are sufficient for a variety of industrial application including not only construction industry where static loading prevails, but also energy industry with dynamic loading conditions. Investigation of the cyclic behaviour of low carbon steel is of particular interest for pumping processes in the mining industry. Components of the pumps which are used for transferring abrasive slurries are subject to fatigue conditions in severe environments. In order to improve performance and optimise the fatigue and corrosion-fatigue life of the high pressure components, an application of compressive residual stress methods such as autofrettage and deep rolling is required.

A compressive residual stress field is induced through a plastic overload of a component. The standard autofrettage procedure suggests a single application of the autofrettage pressure with a subsequent unloading. However, the research made by Farrahi et al. [1], Parker and Huang [2] and Jahed et al. [3] shows that repetitive application of the overload pressure can increase the level of compressive residual stresses, thereby increasing fatigue life of a component. The deep rolling procedure is based on pressing the target surface by roller or ball-point tools cyclically across the component surface in order to induce compressive stresses in the external layers. The phenomenon of cyclic plasticity is therefore essential for the above mentioned residual stress induction procedures. This in turn means that an accurate prediction of the residual stress field requires precise modelling of the cyclic plasticity behaviour which should be based on thorough experimental investigation and advanced theoretical approaches.

✉ Corresponding author (e-mail: volodymyr.okorokov@strath.ac.uk)
* Department of Mechanical & Aerospace Engineering, University of Strathclyde, Glasgow G1 1XJ, UK
† Weir Minerals, Venlo, 5928 PH, the Netherlands

This study involves the phenomenon of mixed cyclic softening and hardening which occurs under the cyclic plasticity conditions. The phenomenon can be observed as a change of stress at a certain strain level under cyclic conditions when compared to the same stress obtained after simple monotonic tension or compression test. Usually materials show either softening or hardening behaviour when the stresses can only decrease or increase appropriately within the entire strain range. However, some materials, particularly low carbon steel, can demonstrate the mixed softening and hardening (Xu et al. [4]). Although cyclic hardening can only take place when stress amplitude exceeds the yield point of the material, cyclic softening can occur even below the point of plastic yielding (Milella [5]). Consideration of the mean stress relaxation in cyclic plasticity is also covered by present study as the effect of non-zero mean strain cycling is in particular interest of the re-autofrettage and deep rolling procedures.

This work presents the constitutive model of plasticity based on the concept of internal variables within the framework of rate-independent plasticity. In order to capture the above mentioned cyclic plasticity phenomena, a new set of internal variables is developed and incorporated into the combined nonlinear kinematic-isotropic hardening model. The new model can provide a better accuracy for both cyclic and monotonic material response. Other phenomena attributed to cyclic loading conditions, such as ratcheting and mean stress relaxation, can also be simulated by the proposed plasticity model.

CYCLIC PLASTICITY

In order to investigate the cyclic and monotonic plasticity behaviour of low carbon steel, both monotonic and cyclic tests with different loading programs have been conducted. The testing has been done with the use of a 250 kN INSTRON servo-hydraulic testing machine under strain controll with a total strain rate of $5 \cdot 10^{-4}$ s^{-1}. The strain has been measured by an extensometer with 10 mm in gauge length.

The monotonic test has been performed for both tension and compression. In order to investigate the mixed cyclic softening and hardening phenomenon, the cyclic testing has been conducted according to the loading program of increasing and decreasing the strain amplitude. The phenomenon of the cyclic mean stress relaxation has been induced by cyclic tests with non-zero mean strain value. The tests were run until a stabilization of the stress at each level of the strain.

Experimental results

The engineering stress-strain diagram together with the basic material mechanical properties obtained from the monotonic tests are presented in Fig. 1. Figure 2 demonstrates several monotonic stress-strain curves within the 3% of strain range for the samples with both tension and compression loadings. These results show that both tension and compression stress-strain curves remain within a statistical scatter. This fact can simplify modelling the material behaviour by allowing the use of von Mises yield criterion for three dimensional stress-strain state.

From the first sight it looks like the material has elastic behaviour up to the initiation of the plateau on a stress-strain curve. However, Fig. 3a shows that the stress-strain relationships deviate from a linear law much earlier than the initiation of the plateau. It means that even in monotonic loading conditions the material has two yield points which can be called the first and second yield points. The existence of plastic strains which starts just after the first yield point can be clearly seen in Fig. 3b, where the cyclic softening occurs under a constant strain amplitude cycling. It can be also

observed that the mean stress of the stabilized plasticity loop shows a strong dependence on whether the tension or compression was at the first step of loading. Such a behaviour can lead to a different fatigue life as the mean stress can be positive or negative depending on the first step of an applied load. This suggests that the standard low cycle fatigue assessment methods are unable to predict fatigue life as they use the cyclic stress-strain curve which in turn depends on the first steps of loading.

Figure 4 shows the results from the increasing level test (ILT) and decreasing level test (DLT). In order to investigate the relationships between the stabilized stresses and strain ranges, the test has been performed within the strain amplitude range from 0.1 to 2.0%. The results demonstrate that for each strain amplitude the stress peaks change until saturating on a certain value. The observations for decreasing level test are similar to the results of the previous test except for the fact that the stress saturation has a strong dependence on the maximum strain amplitude reached before decreasing a load. Figure 5 demonstrates the cyclic stress-strain curves for various levels of the maximum strain amplitude.

Figure 6 illustrates the results from the test with non-zero mean strain which induces the mean stress relaxation. This test is of a particular interest for the compressive residual stress induction methods as the test can show a realistic material response similar to that from the application of the re-autofrettage and deep rolling procedures. This means that applying the overload pressure several times may lead to a deeper level of compressive residual stresses.

Constitutive modelling

This study presents a constitutive model of cyclic plasticity which is based on the von Mises yield criterion. The yield surface is implemented as follows:

$$\mathrm{f} = \sqrt{\frac{3}{2}(\mathbf{S}-\mathbf{X}):(\mathbf{S}-\mathbf{X})} - \mathrm{R} - \sigma_0 \tag{1}$$

where $\mathbf{S}$ – deviatoric stress tensor; $\mathbf{X}$ - back stress tensor; R - isotropic hardening variable; σ_0 - initial size of the elastic domain.

The phenomena of cyclic softening and hardening suggest that stable hysteresis loops are achieved after a cycling under a fixed strain range. The present experimental observations show a strong dependence between stabilized stress peaks and strain ranges, thereby exhibiting non-Masing behaviour. In order to describe this type of the material behaviour, Chaboche et al. [6] proposed to use a new internal variable which introduces a dependence of the isotropic hardening asymptotic value on the plastic strain range. The memory surface is introduced in the following way:

$$\mathrm{F} = \sqrt{\left(\boldsymbol{\varepsilon}^{\mathbf{p}} - \boldsymbol{\zeta}\right)\left(\boldsymbol{\varepsilon}^{\mathbf{p}} - \boldsymbol{\zeta}\right)} - \mathrm{q} \tag{2}$$

where $\boldsymbol{\varepsilon}^{\mathbf{p}}$ – plastic strain tensor; $\boldsymbol{\zeta}$ and q – the centre and the radius of the memory surface, respectively. The expressions for these variables are first presented in the following way:

$$\dot{\mathrm{q}} = \frac{2}{3}\eta\,\mathrm{H}(\mathrm{F})\left\langle \mathbf{n}:\mathbf{n}^{*}\right\rangle \dot{\mathrm{p}} \qquad\qquad \dot{\boldsymbol{\zeta}} = \frac{2}{3}(1-\eta)\,\mathrm{H}(\mathrm{F})\left\langle \mathbf{n}:\mathbf{n}^{*}\right\rangle \mathbf{n}^{*}\,\dot{\mathrm{p}} \tag{3}$$

where $\mathbf{n}$ – the unit normal; H – the Heaviside function; $\dot{\mathrm{p}}$ - accumulated plastic strain rate;

Nouailhas et al. [7] and Ohno [8] introduced a fading function into the variable q in order to provide a better agreement with experiments. Despite of the fact that these constitutive models are

able to describe a cyclic stress-strain curve quite precisely, there are a few disadvantages of the model. It was noted in [4] that the classical approach considers the change in the peak stresses rather than the variation of the cyclic loops shapes. Moreover, the shape of the monotonic curve as well as the shape of each curve from a cyclic loading is completely determined by a single unified set of equations and parameters calibrated for a cyclic stress-strain curve. This means that even if the cyclic behaviour of peak stresses has a good coincidence with experimental results, both the shape of each curve and saturation effect of peak stresses cannot be modelled properly with the classical approach.

In order to describe every stress-strain curve for cyclic loading starting from the monotonic curve up to the saturation of stresses, a new set of internal variables is proposed in this study. A thorough observation of the results yields into an important conclusion that can be drawn from a phenomenological point of view. With the use of the classical approach, saturation of stresses on a new strain range should start immediately with the transition of the strain amplitude to a new value. However, the experiment shows that the slope of the hardening line does not change until reaching the end of the cycle. This means that there is a parameter that remains unchanged during the entire cycle and starts influencing the material behaviour only at the beginning of the next cycle. Other observations regarding the transition between cycling behaviour below and above yielding plateau or cycling around non-zero mean strain suggest existence of the parameters that keep unchanged during the current cycle of loading and initiate at a new cycle.

In order to reflect the above observation in the constitutive modelling, two new internal variables are introduced in the following form:

$$\dot{\bar{q}} = \left[p - \bar{p}' - 2\bar{q}'\right]\delta(Z)\dot{p} \qquad \dot{\bar{p}} = \left[p - \bar{p}'\right]\delta(Z)\dot{p} \tag{4}$$

where $\dot{\bar{q}}$ stand for the rate of strain amplitude that is attained in the previous step and $\dot{\bar{p}}$ stand for the rate of accumulated plastic strain that is attained during all straining up to the end of the previous step; δ - Dirac delta function the argument of which is defined as follows:

$$Z = \frac{1}{2}\left[p - p' - \mathrm{sign}(\varepsilon_{eq}^{p} - \bar{\varepsilon}_{eq}^{p})(\varepsilon_{eq}^{p} - \varepsilon_{eq}'^{p})\right] \qquad \varepsilon_{eq}^{p} = \sqrt{\frac{2}{3}\boldsymbol{\varepsilon}^{\mathbf{p}} : \boldsymbol{\varepsilon}^{\mathbf{p}}} \tag{5}$$

$$\bar{q}' = \bar{q}(t-\tau) \qquad p' = p(t-\tau) \qquad \bar{p}' = \bar{p}(t-\tau) \qquad \varepsilon_{eq}'^{p} = \varepsilon_{eq}^{p}(t-\tau) \tag{6}$$

where τ - infinitesimal time delay. The main feature of the above delay differential equations is that the Dirac function returns a required value exactly at the beginning of a new step. At other moments of time the Dirac function returns zero value and the variables remain unchanged during the plastic deformation. This allows the new variables to be constants on the current step of loading and change their value only at the beginning of the next step. According to the classical approach the strain range dependence is introduced only into the constant in the isotropic hardening rule:

$$\dot{R} = b(Q - R)\dot{p} \qquad \dot{Q} = \mu(Q_s - Q)\dot{\bar{q}} \qquad \dot{b} = \vartheta(b_s - b)\dot{\bar{q}} \tag{7}$$

where μ, Q_s, ϑ and b_s are material constants. However, present experimental observations show a necessity to incorporate this dependence into the kinematic hardening rule as well. New expressions for isotropic and kinematic hardening rules are presented in the following way:

$$\mathbf{X} = \sum_{i=1}^{m}\mathbf{X}_i \qquad \dot{\mathbf{X}}_i = \frac{2}{3}c_i\gamma_i\dot{\boldsymbol{\varepsilon}} - \gamma_i\mathbf{X}_i\dot{p} \qquad \dot{c}_i = a_i^{c}(A_i^{c} - c_i)\dot{\bar{p}} \qquad \dot{\gamma}_i = a_i^{\gamma}(A_i^{\gamma} - \gamma_i)\dot{\bar{p}} \tag{8}$$

$$\dot{A}_i^c = d_i^c (D_i^c - A_i^c)\dot{\bar{q}} \quad \dot{a}_i^c = g_i^c (G_i^c - a_i^c)\dot{\bar{q}} \quad \dot{A}_i^\gamma = d_i^\gamma (D_i^\gamma - A_i^\gamma)\dot{\bar{q}} \quad \dot{a}_i^\gamma = g_i^\gamma (G_i^\gamma - a_i^\gamma)\dot{\bar{q}} \tag{9}$$

In the modified kinematic hardening rule the functions A_i^c and A_i^γ are responsible for the saturation values of the functions c_i and γ_i respectively, while a_i^c and a_i^γ stand for the rate of the saturation. D_i^c, d_i^c, G_i^c, g_i^c, D_i^γ, d_i^γ, G_i^γ and g_i^γ are material constants and i is a number of components in back stress decomposition. In general, three components are enough to model the shape of the stress-strain curve accurately.

The new modifications allow calibrating the model not only to the monotonic or cyclic stress strain curve at the stabilized state, but also to intermediate stress-strain curves. This is very important for the compressive residual stress induction methods as they require accurate modelling of the first few cycles rather than stabilized stress-strain curves.

There is another experimental observation regarding non-zero mean strain cyclic loading. After the calibration of the proposed plasticity model to the zero mean strain cycling, the resulting stress-strain curves tend to stabilize at zero mean stress value. That is one of the essential attributes of the Chaboche kinematic hardening rule. There is a large number of studies (Lee et al. [9], Chiang [10] and Arcari and Dowling [11]) that use modifications to the constants of the classical model to overcome this problem. In order to reflect these experimental observations, it is convenient to present a kinematic hardening rule in the following form:

$$\dot{\mathbf{X}}_i = \frac{2}{3} c_i \gamma_i \dot{\boldsymbol{\varepsilon}} - \gamma_i \left(\mathbf{X}_i - \mathbf{X}_i^m\right)\dot{p} \qquad \mathbf{X}_i^m = \mathbf{X}_i^{in} - \overline{\mathbf{X}}_i \tag{10}$$

where $\mathbf{X}_i^{in}$ - initial values of back stress tensor components reached in a previous step; $\overline{\mathbf{X}}_i$ - back stress tensor whose components values are reached in the previous step. This modification is a convenient way to present a non-zero mean strain effect as it does not require determination of new constants.

APPLICATION OF PLASTICITY MODEL TO FATIGUE ANALYSIS

The effect of mean stress on fatigue life is investigated experimentally in many studies (Bader and Kadum [12], Svensson et al. [13] and Dowling [14]). In general, positive tensile mean stress leads to a higher fatigue crack growth thereby decreasing the fatigue life of a component. Just an opposite is the effect of negative compressive mean stress. Fatigue tests with negative mean stress show longer fatigue life compared to those with positive mean stress. Therefore, induction of a compressive residual stress in high pressure components has become a useful practice for increasing fatigue life in both air and corrosion environment. Since all compressive residual stress induction methods are based on a plastic overload of a material, the use of realistic plasticity models has a crucial role in predicting the compressive residual stress field in a high pressure component. In this paper the modelling of the autofrettage and re-autofrettage procedure for a benchmark problem is presented.

Simulation of the autofrettage for thick-walled cylinder

The idea of the autofrettage is to apply a high pressure to the internal surface of a high pressure component in order to induce a plastic strain of required values. With unloading the elastic layers of a component start shrinking the plastically deformed layers thereby inducing compressive stresses. Application of the autofrettage pressure several times can increase the magnitude of the compressive

stress. Obtained experimental results shown in Fig. 7 demonstrate that several cycles until reaching the final point can induce a larger magnitude of the compressive stress than a single application of a load. This fact can be used in autofrettage procedures where increasing the autofrettage pressure is applied via a number of steps. It should be noted that a proper modelling of the effect of re-autofrettage is not possible without a plasticity model that can predict cyclic plasticity accurately.

As an example of the beneficial effect of the autofrettage and re-autofrettage procedure a benchmark problem of a high pressure thick-walled tube is considered. The tube is modelled as an axisymmetric endless cylinder with the inner radius of 30 mm and outer radius of 90 mm. In order to model the re-autofrettage, the overloading pressure is applied six times increasing from the minimum value of 280 MPa to the maximum value of 310 MPa with 5 MPa of the increment. The numerical simulation is implemented by means of FEM with the use of ANSYS Workbench. The proposed plasticity model is incorporated into ANSYS Workbench by the means of User Programmable Features (UPF), where user implements custom equations and solving algorithms.

Figure 8 shows the results of the autofrettage and re-autofrettage simulation. Single autofrettage simulation results after applying only the maximum pressure is compared to the re-autofrettage results. The distribution of the hoop stresses demonstrates that the re-autofrettage can increase the magnitude of compressive residual stress near the bore up to 15%. It should be noted that the sequence of applying pressure for the re-autofrettage has been chosen arbitrary. Therefore, a larger improvement can be expected with finding an optimum sequence and values of pressure.

High cycle fatigue assessment

There is a number of multiaxual fatigue criteria for determination of equivalent stress, which is compared to uniaxial experimental data. Such widely used multiaxual criteria as von Mises, Tresca or maximum principal stress criteria have a good experimental agreement for the case of completely reversed loading or loading with positive means stress. Since they return only a positive value for the equivalent stress, the negative compressive mean stress effect cannot be properly modelled by these criteria. In order to assess a negative mean stress effect, the critical plane approach and approach based on proportionality of effective mean stress to hydrostatic pressure presented by Dowling [15] can be used. According to the second approach, the equivalent stress amplitude and mean stress are defined as follows:

$$\sigma_{\mathrm{eq}}^{\mathrm{a}} = \frac{1}{\sqrt{2}}\sqrt{\left(\sigma_{11}^{\mathrm{a}} - \sigma_{22}^{\mathrm{a}}\right) + \left(\sigma_{22}^{\mathrm{a}} - \sigma_{33}^{\mathrm{a}}\right) + \left(\sigma_{33}^{\mathrm{a}} - \sigma_{11}^{\mathrm{a}}\right) + 6\left(\tau_{12}^{\mathrm{a}\,2} + \tau_{23}^{\mathrm{a}\,2} + \tau_{31}^{\mathrm{a}\,2}\right)} \tag{11}$$

$$\sigma_{\mathrm{eq}}^{\mathrm{m}} = \sigma_{11}^{\mathrm{m}} + \sigma_{22}^{\mathrm{m}} + \sigma_{33}^{\mathrm{m}} \tag{12}$$

In order to assess fatigue life of the thick-walled cylinder after the autofrettage, the above fatigue equations are inserted into ANSYS Workbench with the use of UPF in the same way as the plasticity equations. Simulation are performed for both non-autofrettaged and autofrettaged cylinders. Figure 9 illustrates the area of the Haigh diagram with R = -1 and R = 0 for fatigue life of one million cycles according to the experimental data presented by Boller and Seeger [16]. For the case of the non-autofrettaged cylinder with R = 0 type of loading 1 million cycles should be reached when the service pressure equals to 205 MPa. If the autofrettage is used, the service pressure can be increased to the value of 250 MPa to serve the same life as the non-autofrettaged cylinder.

CONCLUSIONS

This paper presents the developments of cyclic plasticity constitutive modelling of low carbon steel based on cyclic plasticity experimental observation. A new set of internal variables is developed and incorporated into the combined isotropic and kinematic hardening rules. Obtained numerical results from cyclic plasticity simulation have a good agreement with experimental data, particularly with modelling the mixed cyclic softening and hardening and mean stress relaxation.

Developed plasticity model is applied to the autofrettage and re-autofrettage procedures simulation. The ability of the model to predict realistic behaviour of the material allows accurate modelling of inducing compressive residual stress in a high pressure component. The model is also capable of indicating the benefit of repeated application of the overload pressure according to the re-autofrettage procedure.

In order to demonstrate a beneficial effect of the compressive residual stress on fatigue life of high pressure cylinder the fatigue assessment with multiaxual criterion based on proportionality of effective mean stress to hydrostatic pressure is performed. Obtained numerical results show a potential increase of service pressure up to 18%.

REFERENCE LIST

(1) Farrahi, G., Voyiadjis, G., Hoseini, S. and Hosseinian, E., Int. J. Pressure Vessels and Piping, Vol. 98, 2012, pp. 57–64.

(2) Parker, A. and Huang, X., Int. J. Pressure Vessel Technology, Vol. 129, 2007, pp. 83–88.

(3) Jahed, H., Moghadam, B. and Shambooli, M., Int. J. Pressure Vessel Technology, Vol. 128, 2002, pp. 223–226.

(4) Xu, L., Nie, X., Fan, J., Tao, M. and Ding, R., Int. J. Plasticity, Vol. 78, 2016, pp. 44–63.

(5) Milella, P., Fatigue and Corrosion in Metals, Springer, Rome, Italy, 2013.

(6) Chaboche, J., Dang-Van, K. and Cordier, G., Modelisation of the strain memory effect on the cyclic hardening of 316 stainless steel, S.M.I.R.T. 5 Division L, Berlin, Germany, 1979.

(7) Nouailhas, D., Cailletaud, G., Policella, H., Marquis, D., Dufailly, J., Lieurade, H., Ribes, A. and Bollinger, E., Engineering Fracture Mechanics, Vol. 21, No. 4, 1985, pp. 887–895.

(8) Ohno, N., J. Applied Mechanics, Vol. 49, 1982, pp. 721–727.

(9) Lee, C., Do, V. and Chang, K., Int. J. Plasticity, Vol. 62, 2014, pp. 17–33.

(10) Chiang, D., Applied Mathematical Modelling, Vol. 32, 2008, pp. 501–513.

(11) Arcari, A. and Dowling, N., Int. J. Fatigue, Vol. 42, 2012, pp. 17–33.

(12) Bader, Q. and Kadum, E., Int. J. Engineering & Technology, Vol. 14, 2014, pp. 50–58.

(13) Svensson, T., Int. J. Fatigue, Vol. 14, 2003, pp. 50–58.

(14) Dowling, N., Society of Automotive Engineers, DESM, U.S.A., Report No. F2004/51, 2004.

(15) Dowling, N., Mechanical Behavior of Materials, Pearson, Essex, England, 2013.

(16) Boller, C. and Seeger, T., Materials Data for Cyclic Loading, Elsevier, Amsterdam, The Netherlands, 1987.

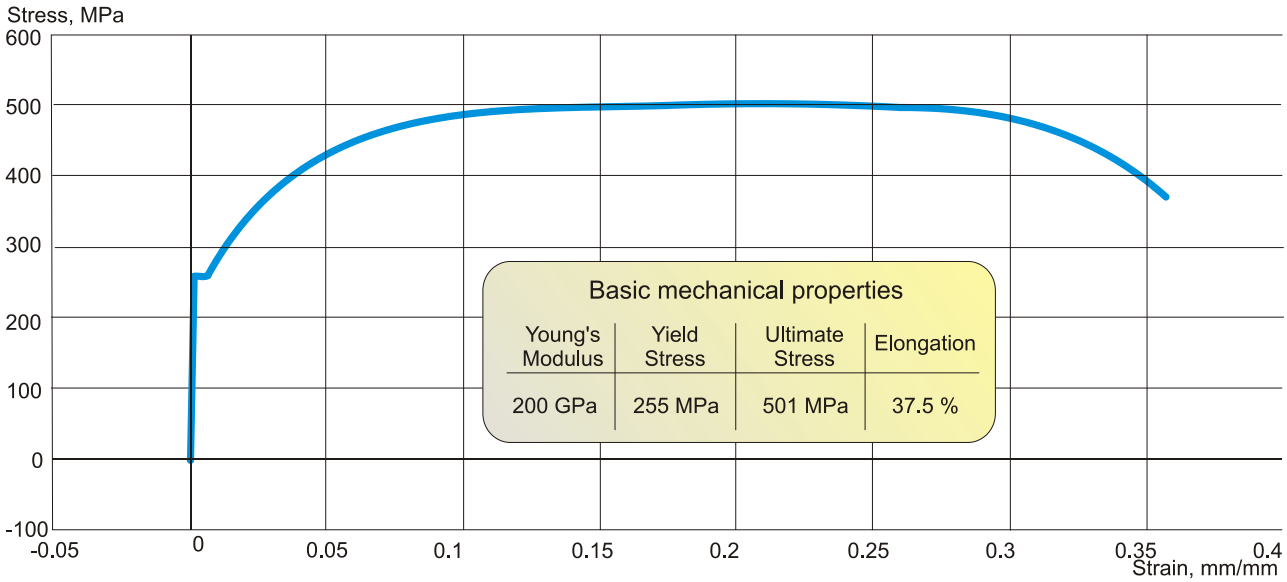

FIGURE 1 Monotonic stress-strain curve and basic mechanical properties of low carbon steel

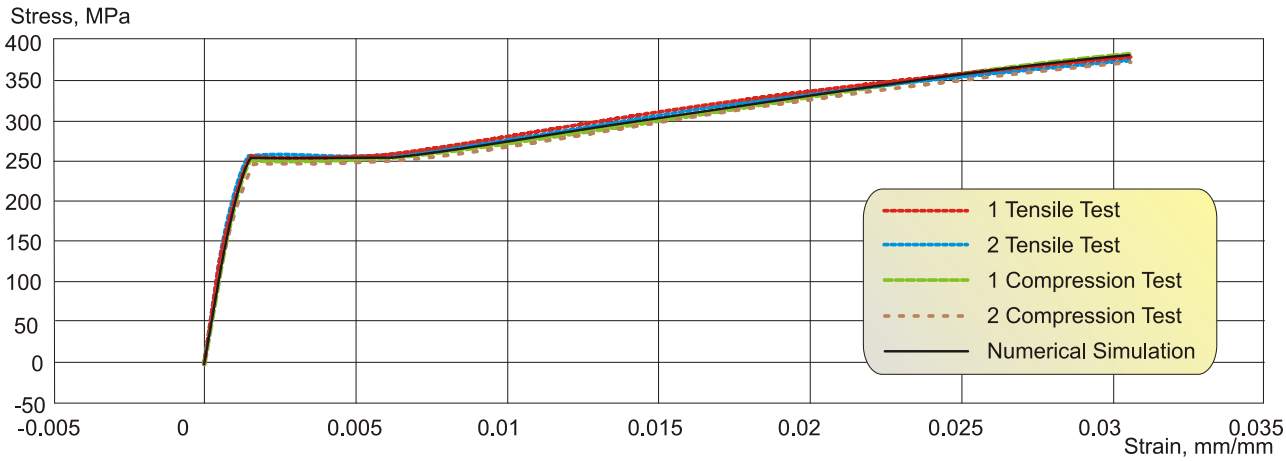

FIGURE 2 Tensile and compression monotonic stress-strain curves

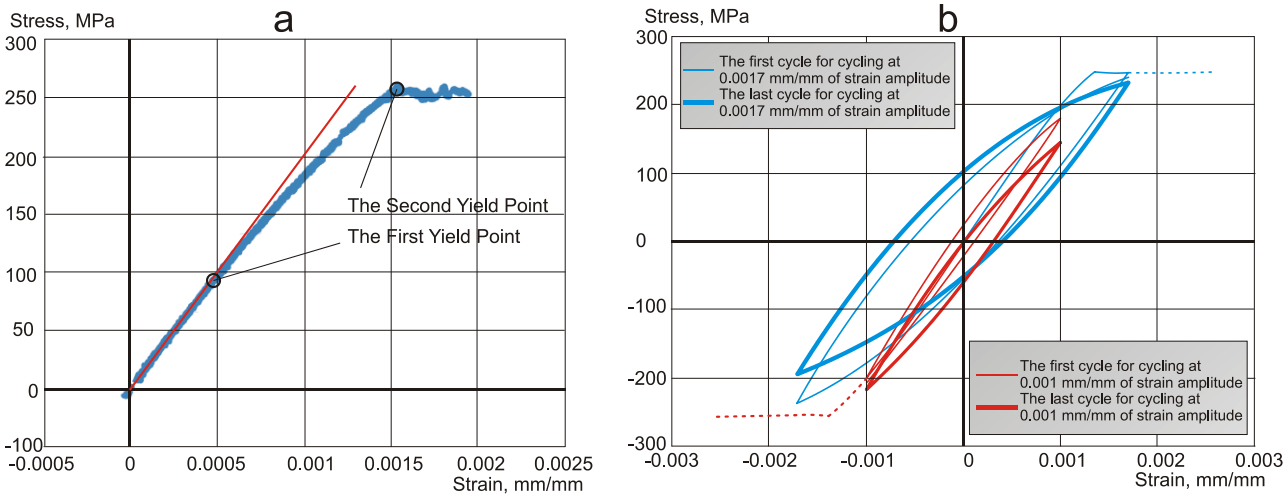

FIGURE 3 Cyclic softening; a) existence of two yield points; b) plasticity loops

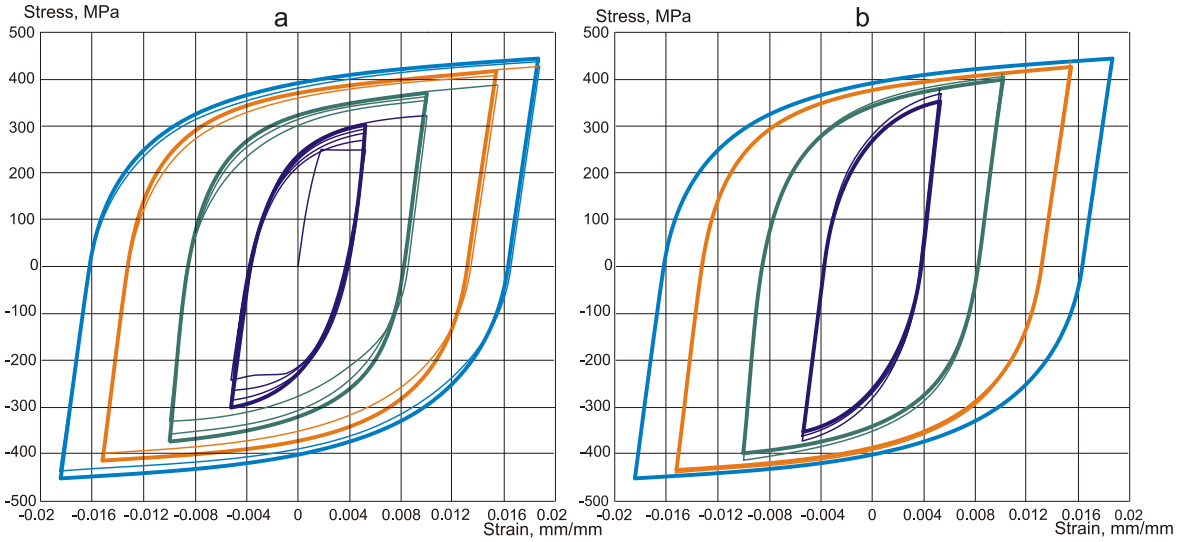

FIGURE 4 Results of a) ILT and b) DLT

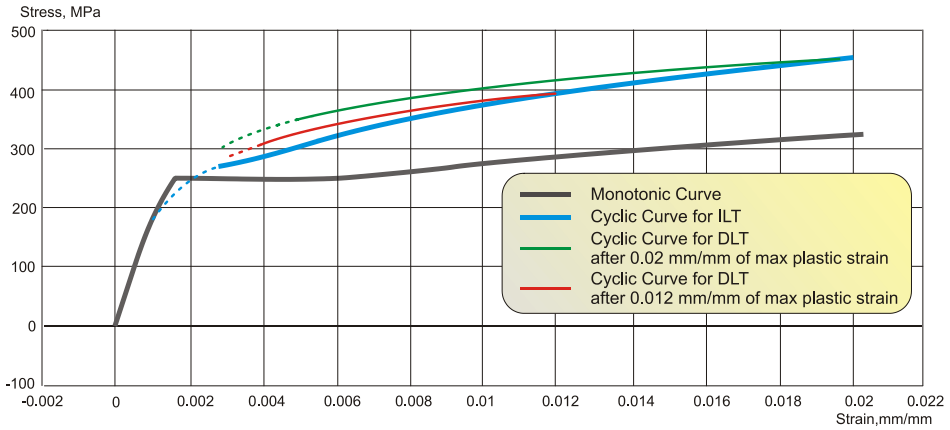

FIGURE 5 Monotonic and cyclic stress-strain curves

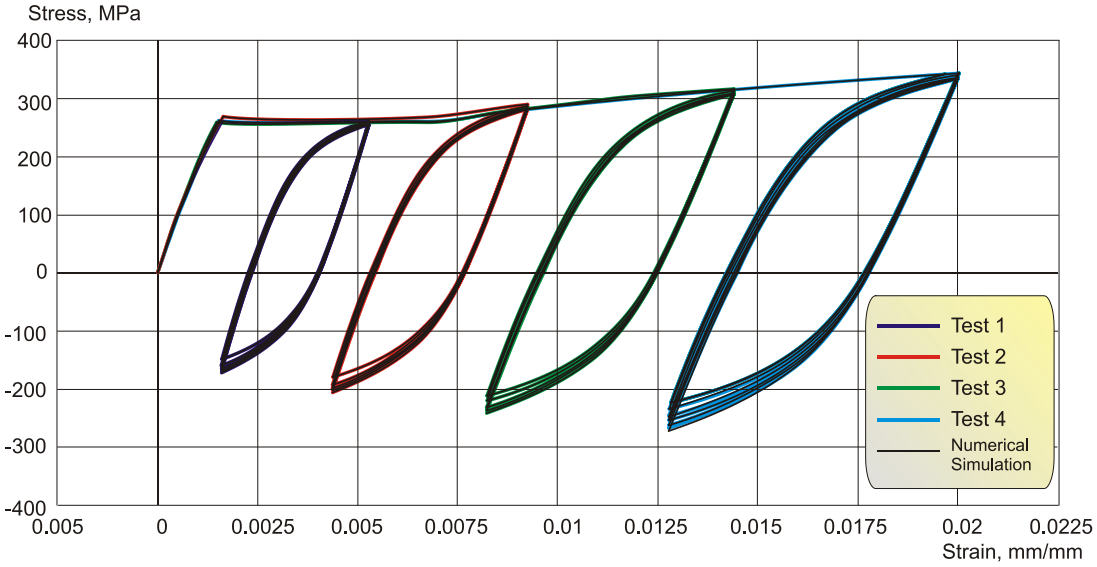

FIGURE 6 Results of cyclic mean stress relaxation test

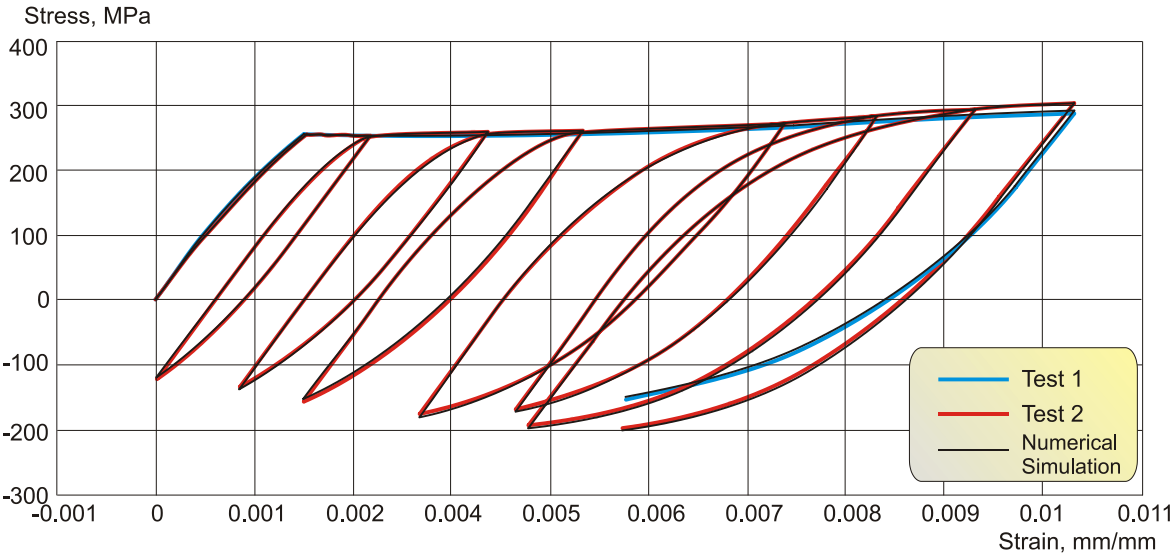

FIGURE 7 Comparison between the results for single and repetitive application of load

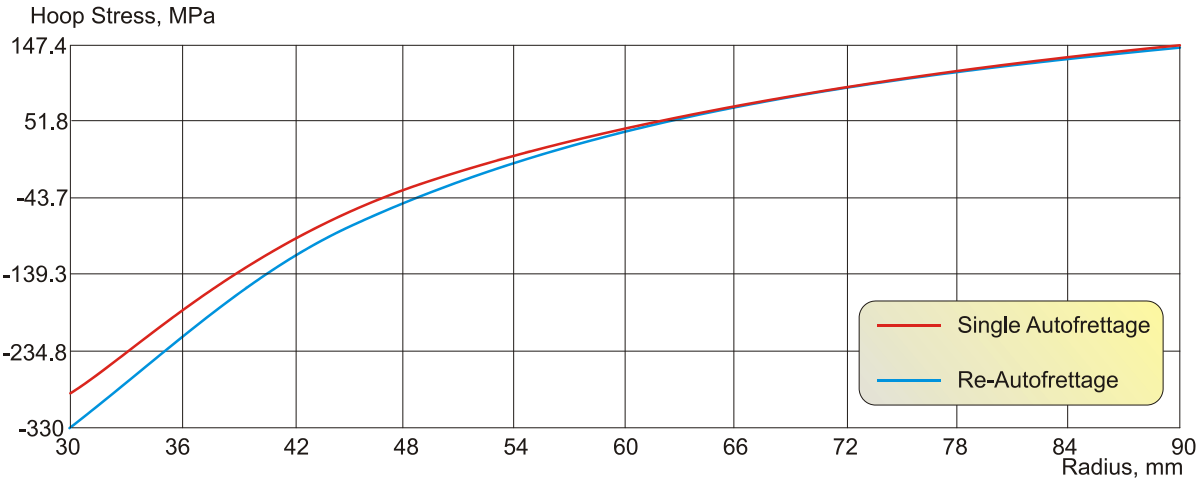

FIGURE 8 Distribution of hoop stress over the radius of the cylinder

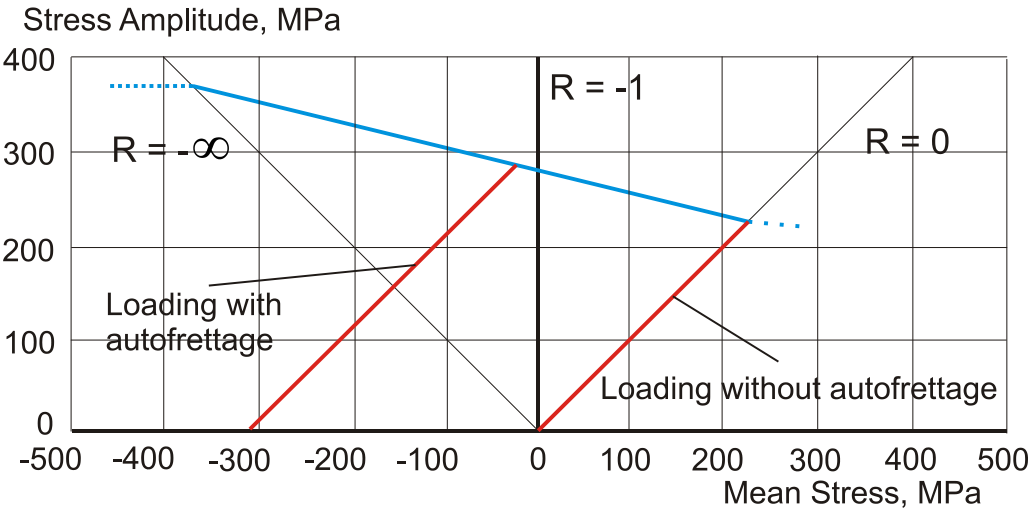

FIGURE 9 Haigh diagram for the cylinders with and without autofrettage